Eur. Phys. J. Special Topics **226**, 1765–1775 (2017)

DOI: 10.1140/epjst/e2017-70041-y

THE EUROPEAN PHYSICAL JOURNAL SPECIAL TOPICS

Regular Article

A system governed by a set of nonautonomous differential equations with robust strange nonchaotic attractor of Hunt and Ott type

Valentina M. Doroshenko[1,a] and Sergey P. Kuznetsov[1,2,b]

[1] Chernyshevsky Saratov State University, Astrakhanskaya, 83, Saratov, 410012, Russia
[2] Kotelnikov Institute of Radio-Engineering and Electronics, Saratov Branch, Zelenaya, 38, Saratov, 410019, Russia

Received 5 February 2017 / Received in final form 8 March 2017
Published online 21 June 2017

Abstract. A physically realizable nonautonomous system of ring structure is considered, which manifests a robust strange nonchaotic attractor (SNA), similar to the attractor in the map on a torus proposed earlier by Hunt and Ott. Numerical simulation of the dynamics for the corresponding non-autonomous set of differential equations with quasi-periodic coefficients is provided. It is demonstrated that in terms of appropriately chosen phase variables the dynamics is consistent with the topology of the mapping of Hunt and Ott on the characteristic period. It has been shown that the occurrence of SNA agrees with the criterion of Pikovsky and Feudel. Also, the computations confirm that the Fourier spectrum in sustained SNA mode is of intermediate class between the continuous and discrete spectra (the singular continuous spectrum).

1 Introduction

Nonlinear systems operating in presence of time-dependent external driving are significant in science and technology. When subjected even to a simple harmonic external action, a nonlinear system may behave in a nontrivial way; for example, manifest transitions from regular motions to chaos. If we consider quasi-periodic driving, say, with a superposition of two harmonic signals with irrational frequency ratio, the variety of phenomena broadens, and new phenomena as strange nonchaotic attractors (SNA) can arise. Attractors of this type are not chaotic in the sense that phase trajectories belonging to them do not manifest exponential sensitivity to initial conditions, i.e., they have no positive Lyapunov exponents, but at the same time the attractor structure in the phase space is characterized by fractal properties [1,2]. For the first time such objects were introduced in consideration in 1984 [1]. Since that time, attractors of this type were found to be quite widespread in quasi-periodically driven systems and studied theoretically and numerically [3–18], and experimentally [19–28]. Despite

[a] e-mail: vvolk92@mail.ru
[b] e-mail: spkuz@yandex.ru

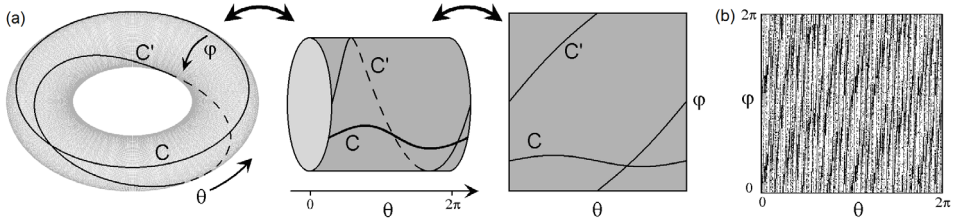

Fig. 1. Schematic representation of a single iteration of the map (1) illustrating the transformation of a closed curve C to the curve C′ (a) and phase portrait of SNA in the map (1) with $F(\varphi,\theta)=\sin 2\varphi$, $\rho=(\sqrt{5}-1)/2$, $\eta=0.5$ (b).

this, it is necessary to note, that there is still not offered a completely satisfactory method to diagnose the presence of SNA in numerical calculations definitively. In fact, all known numerical approaches do not guarantee rigorously that the attractor is strange, that is, retains a fractal structure in arbitrarily small scales.

Usually, the structure of SNA is very sensitive to parameter variations, as they occur close to the boundary between regular and chaotic dynamics [2]. The corresponding regions in parameter space have complicated structure, and small changes in the control parameter may be accompanied with transformation of the SNA into a smooth torus or into a strange chaotic attractor.

In this context, of special interest is a particular kind of SNA introduced by Hunt and Ott [15,16]. Originally, it relates to a discrete-time dynamical system represented by a quasi-periodically driven map on the torus with certain topological properties. In this case it appears to be possible to prove rigorously assertions on the nature of the attractor as SNA. Moreover, assuming a fixed irrational ratio of the basic frequencies, the attractor is characterized by the property of robustness, that is, the dynamics are not sensitive to the specific choice of parameter values, and a concrete form of the map.

The model proposed by Hunt and Ott [15] is defined by the equations

$$\begin{aligned}\varphi_{n+1}&=\varphi_n+\theta_n+\eta F(\varphi_n,\theta_n)\ (\mathrm{mod}2\pi),\\ \theta_{n+1}&=\theta_n+2\pi\rho\ (\mathrm{mod}2\pi),\end{aligned}\tag{1}$$

where $F(\varphi_n,\theta_n)$ is a continuous smooth function having period 2π in both arguments, η is parameter of nonlinearity, ρ is an irrational parameter characterizing the frequency ratio of the external driving to the natural unit frequency of rhythm of the discrete-time iterations. As a particular example, consider the map (1) with nonlinear function $F(\varphi,\theta)=\sin 2\varphi$ and define the frequency parameter by an irrational $\rho=(\sqrt{5}-1)/2$ (the inverse golden mean). According to analysis of Hunt and Ott, the fundamental reason for occurrence of the robust SNA is the topological nature of the map on the two-dimensional torus (Fig. 1a). Namely, if the pre-image curve C bypasses the torus around the parallel, under the effect of the mapping it is transformed to the image C', which performs one complete revolution around the meridian and one complete revolution around the parallel. With each successive map application, the number of turns of the image around the meridian increases by one; in the limit of large number of the steps this number goes to infinity. Presence of the nonlinear term in the first equation provides the invariant measure on the attractor to be of fractal nature; it can be visualized as shown in Figure 1b, which presents a set of points on the attractor in the plane of variables (θ, φ) as obtained numerically at $\eta=0.3$.

The Hunt–Ott map itself is an abstract construction, and a possibility of occurrence of SNA of this type in realistic systems governed by differential equations is

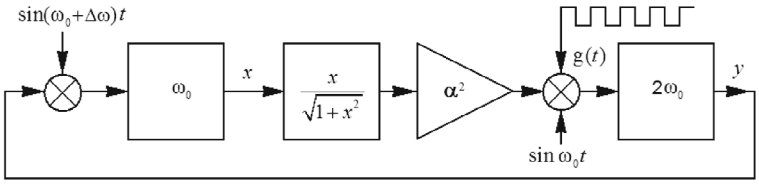

Fig. 2. Block diagram of the system under consideration. The blocks marked ω_0 and $2\omega_0$ are linear second-order filters tuned on the respective frequencies; output signal from the nonlinear element and amplifier (depicted as the triangle) is modulated by period-T pulses of signal of frequency ω_0; also the transmission coefficient of the feedback loop is modulated with the frequency slightly detuned by $\Delta\omega = \pi(\sqrt{5}-1)/T$.

non-trivial. A unique specific example is a non-autonomous system composed of two alternately excited self-oscillating elements proposed and investigated numerically in the work of Kuznetsov and Jalnine [29]. In this paper we consider another implementation of the robust SNA of Hunt and Ott type in a ring system composed of two linear second-order filters and a non-linear amplifying element operating in presence of quasi-periodic modulation of the transmission coefficients with incommensurable frequencies.

2 Description of the system

Consider a system of two linear second-order filters of operating frequencies ω_0 and $2\omega_0$, which are coupled via a nonlinear element and amplifier modulated by periodic pulses of driving signal and closed in a ring with a feedback circuit, providing mixing with external driving signal of frequency slightly shifted comparing to ω_0 (Fig. 2).

The model equations of the system are of the form:

$$\begin{aligned} \ddot{x} + \gamma\dot{x} + \omega_0^2 x &= \varepsilon\alpha^2 \frac{d}{dt}\left[y \sin(\omega_0 t + \theta)\right], \\ \ddot{y} + \gamma\dot{y} + 4\omega_0^2 y &= \varepsilon \frac{d}{dt} \frac{x}{\sqrt{1+x^2}} g(t) \sin\omega_0 t, \\ \dot{\theta} &= \frac{2\pi\rho}{T}, \quad \rho = \frac{\sqrt{5}-1}{2}. \end{aligned} \tag{2}$$

In equations (2) ω_0 is a natural frequency of the first oscillator, while the second has the doubled natural frequency $2\omega_0$; γ is the attenuation coefficient, ε is parameter of coupling, α is gain coefficient of the active element of the circuit. Parameter ρ is defined as the irrational golden mean number as it is traditional in studies of quasi-periodic dynamics; a reason is a convenience of theoretical analysis because of simplicity of presentation of the number by the continued fraction (composed of 1s exclusively).

The effect of the first oscillator to the second is provided by a term represented by a derivative of a product of the non-linear function $\frac{x}{\sqrt{1+x^2}}$ with a reference periodic signal $\sin\omega_0 t$, and a periodic function of modulation $g(t)$ defined as

$$g(t) = \begin{cases} 1, & nT \le t < nT + \tau, \\ 0, & nT + \tau \le t < (n+1)T. \end{cases} \tag{3}$$

It is supposed that both the period T and the pulse duration τ contain integer numbers of periods of the reference high-frequency signal: $T = 2\pi N/\omega_0$, $\tau = 2\pi M/\omega_0$.

The second oscillator affects the first one via the term in the first equation defined as a product of the signal produced by the second oscillator and the reference signal with a frequency shifted (comparing to ω_0) by a constant been in irrational ratio with the modulation frequency $\Delta\omega = 2\pi\rho/T = \rho\omega_0/N$, $\rho = (\sqrt{5}-1)/2$.

Consider briefly the operation principle of the system. Let's start with a time interval, when $g(t) = 0$, supposing the second oscillator to be not excited, while the first oscillator provides damped oscillations at the natural frequency ω_0 with the phase φ: $x \propto \sin(\omega_0 t + \varphi)$. After a while, the factor $g(t)$ becomes nonzero, the second oscillator begins to undergo excitation at the doubled frequency, and the phase shift φ will be transferred as the excitation is determined by the resonant component of the combination $\sin(\omega_0 t + \varphi)\sin\omega_0 t = -\frac{1}{2}\cos(2\omega_0 t + \varphi) + \ldots$ Next, when the initial oscillations of the frequency ω_0 damp in the first oscillator to a negligible level, the second oscillator gets already a sufficiently large amplitude. Now, the first oscillator will accept excitation determined by the product of the signal of the second oscillator and of the reference signal $\cos(2\omega_0 t + \varphi)\sin(\omega_0 t + \theta) = \frac{1}{2}\cos(\omega_0 t + \varphi - \theta) + \ldots$, where the resonant component has the phase $\varphi - \theta$. In fact, the phase φ will accept generally an additional shift (not accounting by the above simple reasoning) determined by some 2π-periodic function of the original phase $f(\varphi)$. As to the phase θ, on the period T it obviously gets a shift $2\pi\rho$. Thus, for the complete period of the external driving T the mapping for the phases will be

$$\begin{aligned} \varphi_{n+1} &= \varphi_n - \theta_n + f(\varphi_n) \bmod 2\pi, \\ \theta_{n+1} &= \theta_n + 2\pi\rho \bmod 2\pi, \end{aligned} \tag{4}$$

and it just corresponds to the form of the Hunt and Ott map (1) (up to non-relevant sign change at θ in the first equation).

3 Results of numerical simulation

Equations (2) alternatively may be rewritten as a set of equations of the first order:

$$\begin{aligned} \dot{x} &= u + \varepsilon y(\cos\theta \sin\,\omega_0 t + \sin\theta \cos\,\omega_0 t), \\ \dot{u} &= -\gamma\dot{x} - \omega_0^2 x, \\ \dot{y} &= v + \varepsilon\alpha^2 \frac{x}{\sqrt{1+x^2}} g(t)\sin\omega_0 t, \\ \dot{v} &= -\gamma\dot{y} - 4\omega_0^2 y, \\ \dot{\theta} &= \frac{2\pi\rho}{T}, \quad \rho = \frac{\sqrt{5}-1}{2}. \end{aligned} \tag{5}$$

Figure 3 shows the time dependencies $x(t)$, $y(t)$ on 10 modulation periods obtained from numerical integration of the system (5) by the Runge–Kutta 4th order method for two sustained oscillatory regimes corresponding to the gain parameters $\alpha = 5$ and 10. Other parameters are fixed:

$$\omega_0 = 6\pi, \quad \tau = 3, \quad T = 6, \quad \gamma = 0.25, \quad \varepsilon = 0.7. \tag{6}$$

Using the data of the numerical simulation, we can verify that the evolution of the phases corresponds to mapping of the same topological class as the model of Hunt and Ott [15,16]. To do this, in the process of the numerical integration we evaluate the phase φ_n of the first oscillator for a discrete sequence of time instants

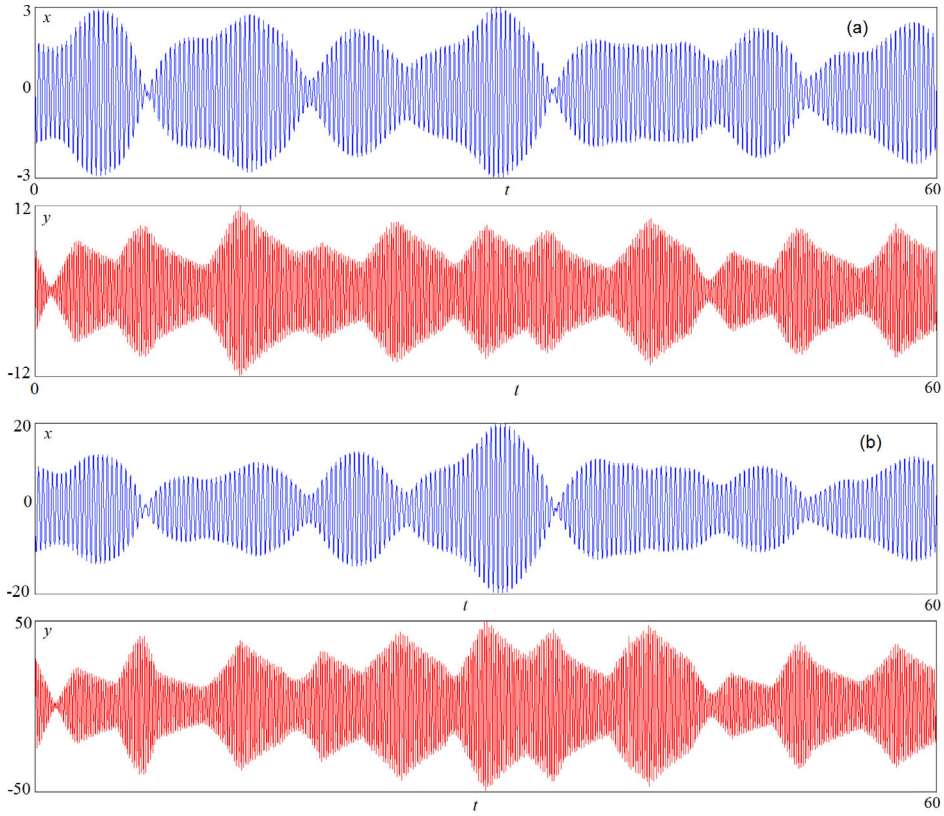

Fig. 3. Time dependences of signals x and y produced, respectively, by the first and the second oscillators at $a = 5$ (a) and $a = 10$ (b) and other parameters assigned according to (6).

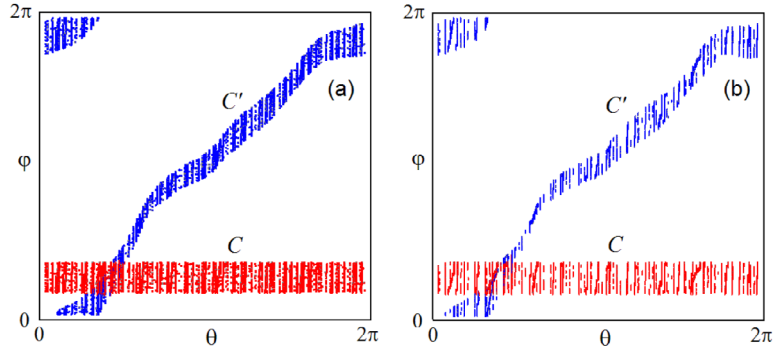

Fig. 4. Numerically obtained illustration of the basic topological properties of phases at $a = 5$ (a) and $a = 10$ (b). Other parameters correspond to (6).

$t_n = nT$ as $\varphi_n = \arg(x(t_n) + i\omega_0^{-1}u(t_n))$. Simultaneously, we calculate the values of $\theta_n = \theta(t_n)\,(\mathrm{mod}2\pi)$. If the obtained φ_n falls into a certain range (of arbitrarily chosen width $\pi/10$), we plot the point θ_n, φ_n on the diagram, and also mark the point θ_{n+1}, φ_{n+1} relating to the instant of time T later. The resulting picture may be interpreted as the torus sweep assuming that the upper and lower sides of the rectangular are identified with the left and right sides, respectively.

Figure 4 shows the results of the numerical data processing for the phases for $a = 5$ and 10 with other parameters (6). In the figure a strip C is seen, formed by the

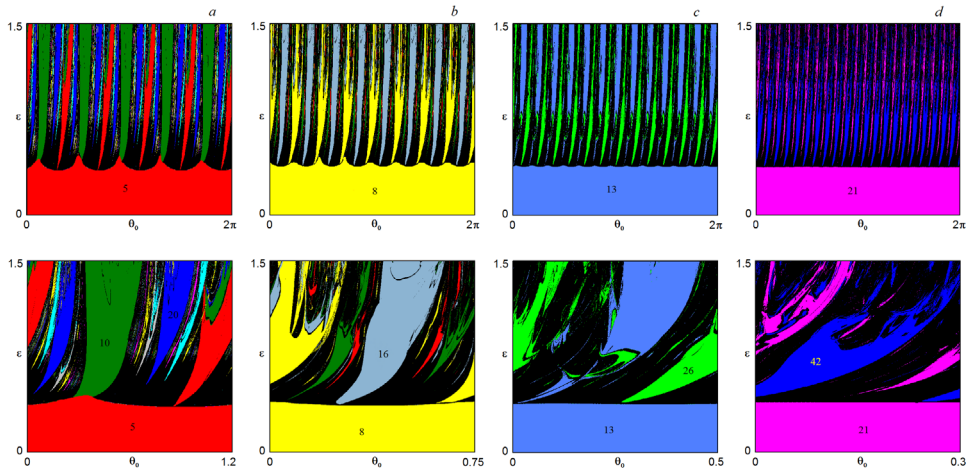

Fig. 5. Charts of dynamical regimes for rational approximations of the frequency ratio ρ_k: (a) 3/5; (b) 5/8; (c) 8/13; (d) 13/21. Periods of the dynamical regimes are indicated inside of the colored domains in the charts in units of period T.

points θ_n, φ_n, and the strip C' is composed of the points θ_{n+1}, φ_{n+1}. The location of these strips indeed corresponds to what expected for a map of the Hunt and Ott class. Namely, the strip C going around the torus along the parallel θ is transformed to the C', which completes one revolution along the meridian and one along the parallel.

4 Rational approximants and the Pikovsky-Feudel criterion

To confirm strange nonchaotic nature of the attractor in our system it is worth turning to verification of the criterion proposed in due time by Pikovsky and Feudel [2,7]. According to their arguments, a necessary condition for existence of SNA is that if one uses rational approximants for the frequency ratio, the system must show bifurcations depending on the initial phase parameter, supposing that this property is retained with increase of the order of the rational approximations.

For the frequency ratio given by the inverse golden mean $\rho = (\sqrt{5} - 1)/2$ the rational approximants are ratios of the successive Fibonacci numbers, namely, $\rho_k = p_k/q_k = F_k/F_{k+1}$, where $F_0 = 0$, $F_1 = 1$, $F_{k+1} = F_{k-1} + F_k$.

If we take the kth approximant instead of the irrational ρ, setting $\rho_k = p_k/q_k$, the external driving will be periodic, with a period $q_k T$. In contrast to the quasi-periodicity with the irrational ρ, when the phase variable θ attends a dense set in the 2π interval in ergodic way, it bypasses now a finite set of points $\{\theta_0, \theta_1, \ldots, \theta_{q_k}\}$. The initial phase θ_0 in this situation must be regarded as an additional parameter; depending on its choice, one can generally obtain various types of dynamics and attractors.

Qualitatively, thinking in terms of rational approximations, one can imagine that the irrational value of the frequency gives rise to a kind of slow drift of the initial phase parameter, and if the system in the course of the dynamics currently is undergoing bifurcations, it just will correspond to the occurrence of SNA [2,7]. Figure 5 shows charts of dynamical regimes depicted on the parameter plane ε, θ_0 with other parameters $\omega_0 = 6\pi$, $\tau = 3$, $T = 6$, $\gamma = 0.25$. Figure 6 shows bifurcation diagrams corresponding to passage along horizontal paths on the charts at two fixed values of $\varepsilon = 0.9$ and 0.11.

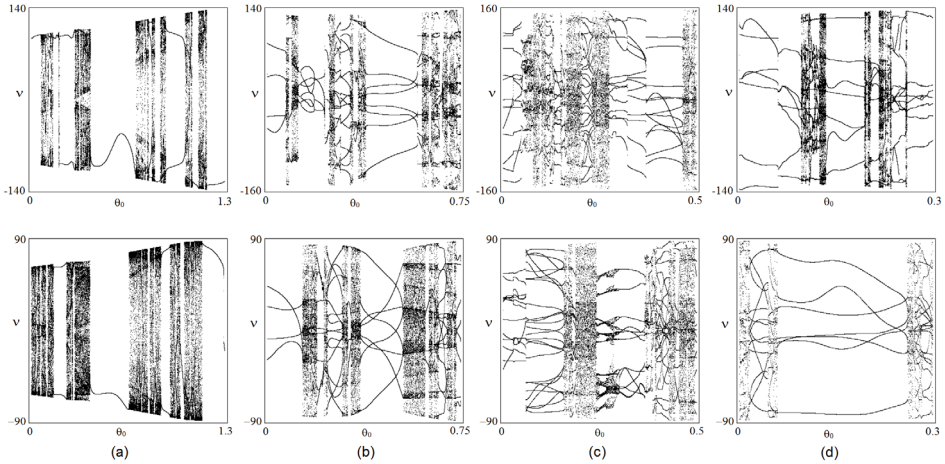

Fig. 6. Bifurcation diagrams obtained for rational approximations of the frequency ratio ρ_k: (a) 3/5; (b) 5/8; (c) 8/13; (d) 13/21 at $\varepsilon = 1.1$ (top row) and $\varepsilon = 0.9$ (bottom row).

Looking at the charts of Figure 5 one can observe that for small values of ε the dynamics are regular, with periods equal to the denominators of the rational approximants, and no bifurcations occur. In contrast, in the top parts of the pictures, roughly, above a certain critical level of ε, the bifurcations take place, and they do not disappear with increasing order of the rational approximations. The bifurcations are accompanied by emergence of regimes of different periods, which are multiples of the denominators of the rational approximations. The same is evident from the bifurcation diagrams shown in Figure 6.

5 Attractor portraits and Lyapunov exponents

Figure 7 in the left part shows three-dimensional stroboscopic portraits of attractors of the system built for two values of the parameter $a = 5, 10$; the dots are plotted with the period of T. Observe that the attractors are characterized by non-uniform subtle structure, which is an attribute of SNA and is not characteristic for smooth tori. In the right part of Figure 7 the same attractors are shown in two-dimensional projection on the plane of phase variables (θ, φ). These diagrams allow judging about fractal distribution of the invariant measure corresponding to the attractors in projection on the torus. It is clearly seen that the distribution is not uniform but manifests wrinkled, fibrous structure formed by regions visiting by the representative point more or less often. Considering enlarged fragments, one can see that this fibrous fractal structure is preserved and reveals more subtle details. Note the evident visual similarity of these pictures to those obtained for the SNA systems of Hunt and Ott type [15,16,29].

Figure 8 shows a graph of Lyapunov exponents depending on the parameter α. The calculations were performed for the system (5) using a standard algorithm [30–32]. This system does not have a positive Lyapunov exponent; the largest one is identically equal to zero (it corresponds to a shift perturbation for the phase variable θ and is not shown on the diagram). The remaining four exponents, as seen from the diagram, are negative. For SNA of Hunt and Ott type, because of its robustness, the dependence of the Lyapunov exponents on the control parameter is smooth. The graph clearly shows that this property holds for the system we discuss in this paper.

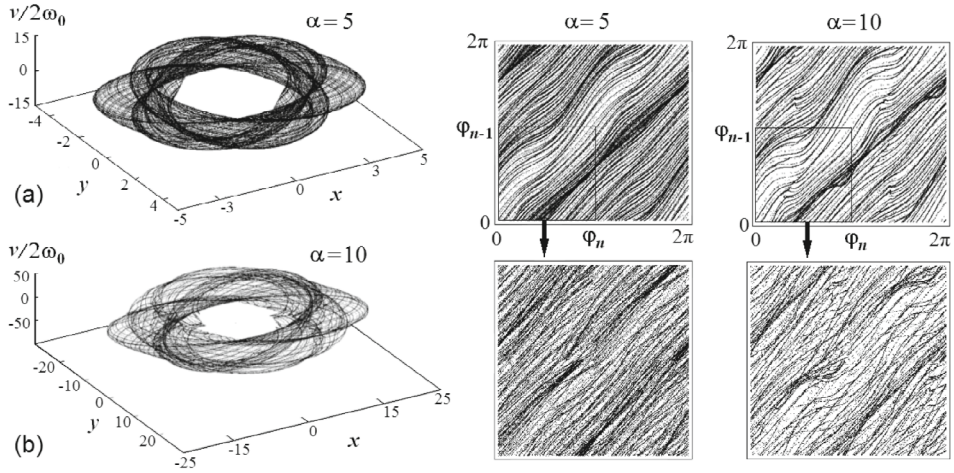

Fig. 7. Stroboscopic portraits of attractors of the system at $a = 5$ (a) and 10 (b) in three-dimensional projections and in two-dimensional representation on the plane of phase variables.

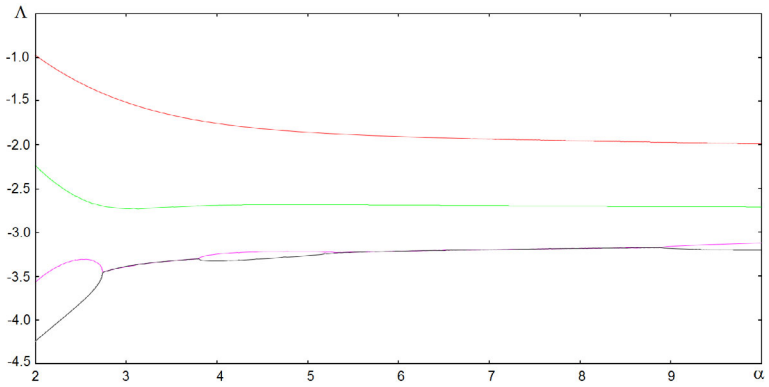

Fig. 8. Graph of Lyapunov exponents, depending on the parameter α; other parameters correspond to (6).

6 Spectral properties of the SNA

Fourier analysis is one of the conventional signal processing techniques in studies of dynamical processes. Of great interest are spectral properties of SNA [2,6,8].

To make clear the specifics of spectral characteristics intrinsic to dynamics of different types, consider construction of the Fourier transform in application to a time series x_n as a process of accumulating for sums:

$$Z(\Omega, N) = \sum_{n=0}^{N-1} x_n e^{i\Omega n}, \tag{7}$$

where n is the discrete time, Ω is a frequency parameter for the spectral component we are interested with, and N is a number of terms in the sum.

For periodic and quasi-periodic dynamics, which correspond to discrete spectra, the cumulating sums with increasing N behave linearly: $|Z| \propto N$, if Ω is equal to a

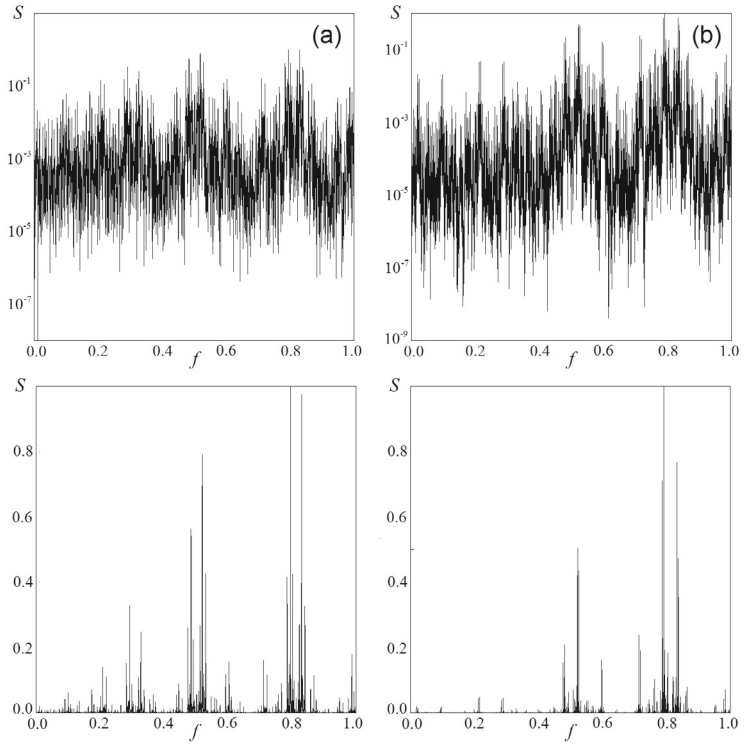

Fig. 9. Fourier spectra for signals produced by the system at $\alpha = 5$ (a) and 10 (b) in logarithmic scale (the top row) and in linear scale (the bottom row).

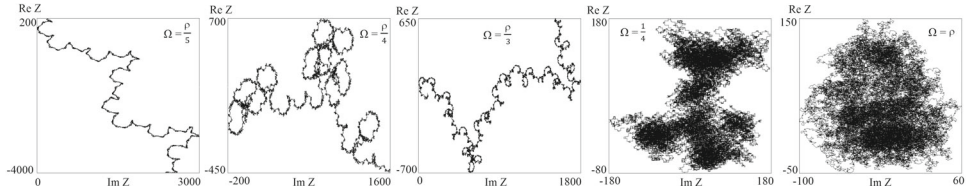

Fig. 10. The walks of the spectral sums on the complex plane for different values of the parameter Ω.

frequency of spectral component presenting in the spectrum, or tend to zero otherwise. For random signals, for arbitrary choice of the parameter Ω, the point representing the cumulating sum will undergo a random walk in the complex plane Z with growing N; it corresponds to linear increase of the mean square of the modulus, so, $|Z| \propto \sqrt{N}$. This is a situation of the continuous spectrum mathematically analyzed in a frame of the Wiener-Khinchin theory. In contrast to these traditionally considered behaviors, for SNA the cumulating sums exhibit a distinct kind of dependences on N, characterized generally by fractional exponents, and it is associated with the so-called singular continuous spectra [2,6,8].

Figure 9 shows Fourier spectra obtained in the numerical calculations for SNA modes of the system (5) in logarithmic and linear scales.

In order to characterize nature of the spectra within the framework of the above considerations, let's turn to diagrams shown in Figure 10, which illustrate graphically

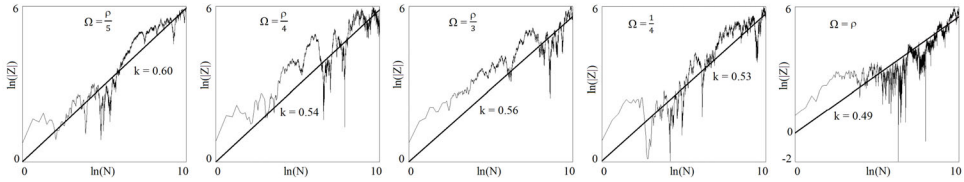

Fig. 11. Estimate of the exponents of the growth of spectral sum modules for different values of the parameter Ω.

the walk of the complex accumulating sums Z_n as obtained from step-by-step computations according to (7). The resulting are non-trivial pictures with evident fractal structure. The graphs are plotted for several different values of the parameter Ω: $\rho/5$, $\rho/4$, $\rho/3$, $1/4$, $1/\rho$. One can observe a "fractal drift", which does not match simple behaviors of growth with the exponents 1 or 1/2, which would correspond to traditional discrete or continuous spectra.

For quantitative characterization of the behavior of the spectral sums we build plots of the modulus $|Z(\Omega, N)|$ depending on the number of terms in the sum N, using the double logarithmic scale. Then, the slope coefficient for a straight line approximating the dependence is an estimation of the respective nontrivial exponent.

The diagrams are shown in Figure 11. The straight lines on the plots indicate the approximations to estimate the slope coefficients. The slopes for periodic and quasi-periodic oscillations would be close to 1, and for a random process or for chaotic oscillations to 1/2. In the case of SNA the exponent estimates give some fractional values, distinct from 1 and 1/2, and different for different frequency parameters Ω. This indicates that we are dealing with the singular continuous spectra [2].

7 Conclusion

The article proposes a realizable system implementing SNA of Hunt and Ott type in a ring circuit composed of a pair of linear second-order filters (oscillators) and a non-linear active amplifying element, with modulation of the transfer coefficients. In such a system the external driving is quasi-periodic and contains basic frequencies that are in irrational ratio, whereby the existence of SNA becomes possible.

The numerical results are obtained indicating that SNA indeed occurs here of the same type as in the artificially constructed map on torus proposed by Hunt and Ott [15], and in a system based on alternately excited self-oscillating elements by Jalnine and Kuznetsov [29]. This is confirmed by demonstration of the basic topological nature of the map for the phase variables.

Additionally, the presence of SNA is illustrated using the criterion of Pikovsky and Feudel with charts of dynamical regimes and bifurcation diagrams obtained for the rational approximants of the basic golden mean frequency ratio. Also we consider the spectral properties of the SNA in some details. Besides the directly calculated spectra, we analyze and discuss behavior of the spectral sums depending on the number of the terms that indicates the singular-continuous type of generated spectra.

The work of VMD was supported partially by RFBR grant No 16-32-00449.

References

1. C. Grebogi, E. Ott, S. Pelikan, J.A. Yorke, Physica D **13**, 261 (1984)
2. U. Feudel, S. Kuznetsov, A. Pikovsky, *Strange Nonchaotic Attractors. Dynamics between Order and Chaos in Quasiperiodically Forced Systems* (World Scientific, Singapore, 2006), p. 228
3. A. Bondeson, E. Ott, T.M. Antonsen, Phys. Rev. Lett. **55**, 2103 (1985)
4. M. Ding, C. Grebogi, E. Ott, Phys. Lett. A **137**, 167 (1989)
5. M. Ding, C. Grebogi, E. Ott, Phys. Rev. A **39**, 2593 (1989)
6. A.S. Pikovsky, U. Feudel, J. Phys. A: Math. Gen. **27**, 5209 (1994)
7. A.S. Pikovsky, U. Feudel, Chaos **5**, 253 (1995)
8. A.S. Pikovsky, M.A. Zaks, U. Feudel, J. Kurths, Phys. Rev. E **52**, 285 (1995)
9. U. Feudel, A.S. Pikovsky, J. Kurths, Physica D **88**, 176 (1995)
10. P. Pokorny, I. Schreiber, M. Marek, Chaos, Solitons and Fractals **7**, 409 (1996)
11. K. Kaneko, T. Nishikawa, Phys. Rev. E **54**, 6114 (1996)
12. P. Glendinning, Phys. Lett. A **244**, 545 (1998)
13. H. Osinga, J. Wiersig, P. Glendinning, U. Feudel, Int. J. Bifurc. Chaos **11**, 3085 (2001)
14. A. Prasad, S.S. Negi, R. Ramaswamy, Int. J. Bifurc. Chaos **11**, 291 (2001)
15. B.R. Hunt, E. Ott, Phys. Rev. Lett. **87**, 254101 (2001)
16. J.-W. Kim, S.-Y. Kim, B. Hunt, E. Ott, Phys. Rev. E **67**, 036211 (2003)
17. S.-Y. Kim, W. Lim, E. Ott, Phys. Rev. E **67**, 056203 (2003)
18. A.Yu. Jalnine, S.P. Kuznetsov, EPL **115**, 30004 (2016)
19. W.L. Ditto, M.L. Spano, H.T. Savage, S.N. Rauseo, J. Heagy, E. Ott, Phys. Rev. Lett. **65**, 533 (1990)
20. S.T. Vohra, F. Bucholtz, K.P. Koo, D.M. Dagenais, Phys. Rev. Lett. **66**, 212 (1991)
21. T. Zhou, F. Moss, A. Bulsara, Phys. Rev. A **45**, 5394 (1992)
22. K.-P. Zeyer, A.F. Miinster, F.W. Schneider, J. Phys. Chem. **99**, 13173 (1995)
23. W.X. Ding, H. Deutsch, A. Dinklage, C. Wilke, Phys. Rev. E **55**, 3769 (1997)
24. T. Yang, K. Bilimgut, Phys. Lett. A **236**, 494 (1997)
25. Y.H. Yu, D.C. Kim, J.Y. Ryu, S.R. Hong, J. Korean Phys. Soc. **34**, 130 (1999)
26. B.P. Bezruchko, S.P. Kuznetsov, Y.P. Seleznev, Phys. Rev. E **62**, 7828 (2000)
27. D. Sanchez, G. Platero, L.L. Bonilla, Phys. Rev. B **63**, 201306 (2001)
28. A. Vaszlenko, O. Feely, Int. J. Bifurc. Chaos **12**, 1633 (2002)
29. A.Yu. Jalnine, S.P. Kuznetsov, Tech. Phys. **52**, 401 (2007)
30. G. Benettin, L. Galgani, A. Giorgilli, J.M. Strelcyn, Meccanica **15**, 9 (1980)
31. S.P. Kuznetsov, *Hyperbolic Chaos: A Physicist's View* (Higher Education Press: Beijing, Springer-Verlag: Berlin, Heidelberg, 2012), p. 336
32. A. Pikovsky, A. Politi, *Lyapunov Exponents: A Tool to Explore Complex Dynamics* (Cambridge University Press, 2016), p. 285